

Simultaneous Temperature and Species Measurements During Self-Oscillating Burning of HMX

Ching-Jen Tang,* YoungJoo Lee,† and Thomas A. Litzinger‡
Pennsylvania State University, University Park, Pennsylvania 16802

The near-surface species and surface temperature were simultaneously measured during self-oscillatory burning of octahydro-1,3,5,7-tetranitro-1,3,5,7-tetrazocine (HMX). A CO₂ laser was used to heat the propellant surface at atmospheric pressure in argon. A microprobe/triple quadrupole mass spectrometer system was used to measure species profiles, and fine-wire thermocouples were used to measure surface temperature. Oscillations of species, temperature, and burning rate were observed with an average surface temperature of ~633 K and frequency of 4 ± 0.2 Hz. The mole fraction of NO₂, HCN, and triazine oscillated in phase with temperature, whereas the mole fractions of N₂O, CH₂O, and the species at mass 28 were 180 deg out of phase with temperature. NO₂ and CH₂O were the most abundant species followed by HCN, N₂O, H₂O, the species at mass 28, and other species. The production of NO₂ and HCN was favored with an increase in temperature and burning rate, whereas the production of N₂O and CH₂O became more important with a decrease in temperature and burning rate. This was qualitatively in line with the accepted global reaction branches in the condensed phase of HMX. From these data, variations of the mole fractions of NO₂, N₂O, CH₂O, and HCN could be directly related to surface temperature. Analysis of the data indicates that the observed oscillatory burning might be related to multiple-step reactions in the condensed phase.

Introduction

THOUGH steady burning of solid propellants is desirable for the design engineers of rocket motors, the nature of unsteady burning appears to be unavoidable in many cases. The most common unsteady behavior for rocket motors is oscillatory burning at specific frequencies. The oscillatory burning normally can be divided into low-frequency nonacoustic instability and acoustic instability. Low-frequency nonacoustic instability is related to intrinsic properties of propellant combustion, not to the natural acoustic modes of the system. The phenomenon of chuffing observed during the operation of rocket motors is an example of nonacoustic instability. Chuffing is a momentary burning followed by a quench period near atmospheric pressure, and these events might repeat for several cycles. During chuffing, the combustion chamber will experience intermittent pressure spikes. Huggett et al.¹ mentioned that the pressure spikes of chuffing may propel the rocket around in an unpredictable manner during the beginning of launch; thus, low-frequency nonacoustic instability could be very dangerous. Acoustic instability is caused by combustion interaction with acoustic waves in the chamber of a rocket motor. The interaction can cause oscillations of pressure inside the combustion chamber and oscillatory burning of the propellant. Because thrust is a function of pressure inside the combustion chamber of a rocket motor, oscillations of pressure will result in oscillations of thrust and vibration of the rocket motor. Consequently, the rocket motor may deviate from design performance. In extreme cases, the motor may explode. Therefore, understanding the mechanism of unsteady burning is crucial for the design of rocket motors.

Huffington^{2,3} observed chuffing during burning of a cordite charge in a small vented vessel, and found that chuffing would

transform into continuous, but oscillatory, burning when the nozzle size was reduced. References 2–4 describe the chuffing behavior using a model in which a liquid layer was first developed on the surface and was then explosively burned out; the process was repeated for several cycles. The oscillatory-burning processes were governed by a highly exothermic reaction in the condensed phase. However, they did not show how the exothermic reaction and propellant properties affected the oscillatory frequency and amplitude. After the explosion mechanism was published, Librovich and Makhviladze,⁵ as well as Yount and Angelus,⁶ reported similar oscillatory mechanisms. Kooker and Nelson,⁷ Bruno et al.,⁸ and De Luca⁹ calculated instantaneous surface temperature profiles during self-oscillatory burning by assuming a one-dimensional unsteady condensed phase and a quasisteady gas phase. Kooker and Nelson⁷ and De Luca⁹ found that self-oscillatory burning was induced by a large exothermic heat release in the condensed phase. De Luca⁹ and Galfetti et al.¹⁰ explicitly concluded that the frequency of oscillation was solely controlled by the condensed-phase thermal wave relaxation time at the prevailing operating conditions. This conclusion is currently adopted by most of the researchers in the area of propellant instability.

Few experimental data are available during self-oscillatory burning. Recently, Bruno et al.⁸ and Zanotti and Carretta¹¹ have been the most active researchers in this area. In their studies, light emission from the burning surface and the gas phase, gas-phase temperature oscillations, and ion current density in the flame were measured during self-oscillatory burning. They conclude that self-oscillatory burning does exist for most solid propellants, and their experimental results are qualitatively consistent with the theoretical analysis of the thermal wave relaxation time in the condensed phase.

The present study was started as a result of an unexpected observation during simultaneous species and temperature measurements for octahydro-1,3,5,7-tetranitro-1,3,5,7-tetrazocine (HMX). The results showed that oscillatory burning of HMX consistently appeared at a heat flux of 30 ± 5 W/cm². Subsequently, the heat flux of 30 ± 5 W/cm² was used to generate oscillatory burning of HMX for a more detailed study of the oscillations. During oscillatory burning of HMX, instantaneous surface species and temperature were simultaneously measured

Received March 5, 1998; revision received July 1, 1998; accepted for publication Aug. 2, 1998. Copyright © 1998 by the American Institute of Aeronautics and Astronautics, Inc. All rights reserved.

*Postdoctoral Scholar, Department of Energy and Geo-Environmental Engineering.

†Postdoctoral Scholar, Department of Mechanical Engineering.

‡Professor, Department of Mechanical Engineering. E-mail: tal2@email.psu.edu. Member AIAA.

by a microprobe/mass spectrometer system and Pt-Pt 13% Rh thermocouples. The resulting data have several unique merits for the investigation of oscillatory burning of solid propellants. First, compared with flame luminosity traces, the oscillatory surface temperature profile, which was not reported previously by the other researchers, is important for the validation of unsteady models of the HMX propellants. Bruno et al.⁸ and Kooker and Nelson⁷ have calculated the surface temperature profile in their modeling efforts, but neither of them has calculated luminosity of combustion. Therefore, the current temperature profile can be directly used to validate the results of unsteady numerical models. Second, the oscillatory surface species profiles, which have not been obtained previously by the other researchers, can reveal the unsteady chemical processes during self-oscillatory burning. These species measurements also can be used for validation of models with detailed chemical reactions, which recently have drawn much attention.¹² Third, the observed self-oscillatory burning is a typical example of nonacoustic instability, but the current oscillatory data may be applicable to the study of practical acoustic instability of a solid rocket motor. Oberg¹³ and Culick¹⁴ have found that the low-frequency nonacoustic instability can be considered as a special case of the acoustic instability. Yount and Angelus⁶ mentioned that the intrinsic combustion disturbances might couple with the acoustic properties of the motor with a large cavity. Therefore, the current nonacoustic data may be relevant for understanding acoustic instability. In the present study, much effort was devoted to examine the existing unsteady mechanisms and whether or not the chemical reactions in the condensed phase could affect the amplitude and frequency of self-oscillatory burning.

Experimental Procedures

Simultaneous surface species and temperature measurements were performed in the current study. These measurements enabled observation of the relationship between surface temperature and transient species products in the condensed phase. Although the simultaneous species and temperature measurements have not been conducted previously in our laboratory, all of the required equipment was available from previous studies.¹⁵ A schematic diagram representing the experimental setup is given in Fig. 1. The experimental setup has been described in detail,¹⁵ and only a brief overview will be given in

this section. A CO₂ laser was used as an external energy source to induce the decomposition of HMX. The laser was capable of producing 800 W in a continuous wave mode with precise control of the power output and lasing time. Because the CO₂ laser beam passed through a mask and an expanding lens before entering the test chamber, the beam was relatively uniform. A Pulnix charge-coupled device (CCD) camera with a microlens was used to obtain images of the surface structure. The video system could provide a magnification of 30–40 times, corresponding to a spatial resolution of about 20 μm on the videos. A triple quadrupole mass spectrometer (TQMS) and a thermocouple system were used to perform the simultaneous species and temperature measurements.

The test chamber was 25.4 cm tall and 16.5 cm on a side to give an internal volume of 4460 cm³. Because the volume of the test chamber was adequate, significant pressure oscillation was not expected to occur at a burning rate of 0.4 mm/s for a 0.64-cm-diam propellant. Although the chamber has been used to test up to 5 atm, all of the current tests were conducted at atmospheric in gaseous.

Samples

The HMX samples were 0.64-cm-diam pellets pressed from HMX powder that contains 0.2% hexahydro-1,3,5-trinitro-s-triazine (RDX) as an impurity. The sample pellets had a density of 1.7 g/cm³, which is 89% of the maximum theoretical density. To avoid hydration of the samples, they were stored with desiccants prior to use.

Species Measurements

The HMX pellet was attached on a spring-loaded sample holder that was mounted on a programmable linear positioner inserted through the bottom of the test chamber. Prior to a test, the sample was arranged so that the distance between the center of the sample surface and the probe tip was approximately 1 mm. The distance of 1 mm was a compromise between two constraints. First, the probe tip should be as close to the sample surface as possible to avoid possible reactions in the gas phase. Second, the probe tip must be placed a certain distance away from the surface to avoid possible contact between the tip and the dynamic liquid layer on the surface.

The analysis of gaseous species was performed using the TQMS. The species were sampled by quartz microprobes with

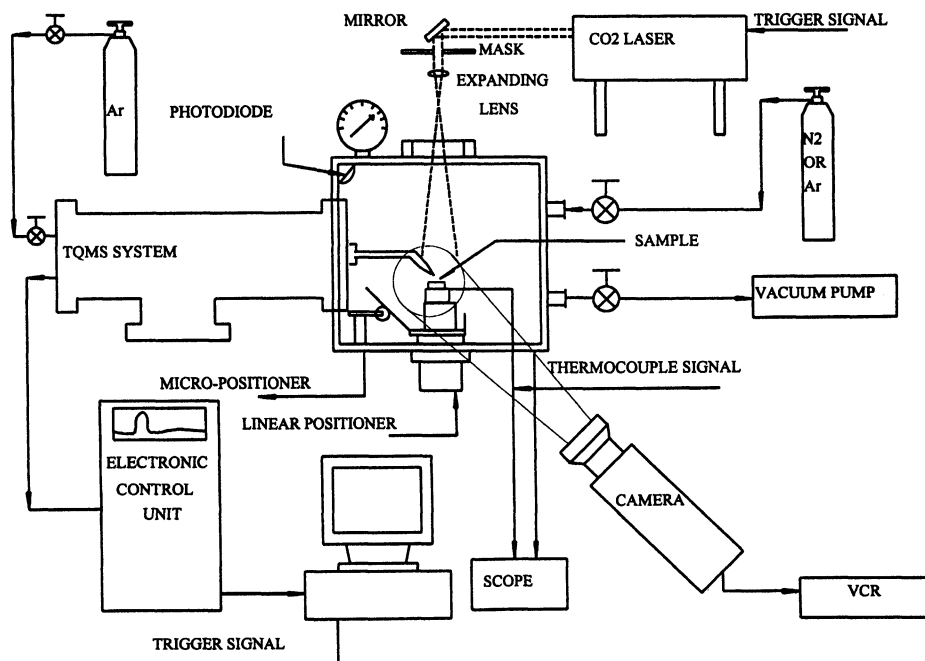
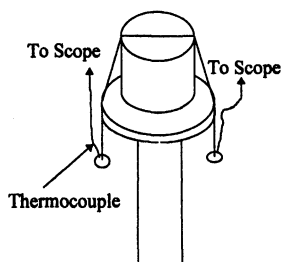


Fig. 1 Overall experimental setup with diagnostic systems.

Fig. 2 Configuration of surface temperature measurements.



an orifice diameter of 20–30 μm , which produced a spatial resolution of 100–150 μm . The sample gases were drawn through the probe into the mass spectrometer by a two-stage pumping system and ionized by electron impact. An ionization energy of 22 eV was used for all of the calibrations and actual tests to minimize fragmentation of molecules and to obtain acceptable intensities. The sample gases can be analyzed in the daughter and parent modes to identify and quantify almost every stable species. In the parent mode of the operation, the species with different molecular weights were readily identified by their unique m/z . In the daughter mode of the operation, the first quadrupole mass filter electromagnetically filtered out the parent ions of the desired m/z and allowed them to pass into the second quadrupole as well as collide with argon gas. Thereby, the ions were fragmented into several pieces, the daughters, because of collision induced dissociation. However, only the parent mode was used in the current study.

Several methods of calibration were used to determine the quantitative species profiles. Because the pressure of the test chamber was very close to 1 atm throughout a test, all of the species were calibrated at atmospheric pressure. Most stable species were calibrated with gas mixtures of known concentration. Species such as water, formaldehyde, and triazine, which are liquid or solid powders at atmospheric pressure and room temperature, were calibrated through another procedure. For example, water vapor was obtained by heating a small cup of liquid water, under the probe with the CO_2 laser in an argon environment. As a result, the gas mixture entering the probe only contained water and argon. Because the calibration factor for argon was obtained in advance by calibrating the known concentration of argon, the calibration factor for water could be readily obtained. The formaldehyde and triazine powder were purchased from Aldrich. The calibrations of species for which standards were not readily available, e.g., hydrogen cyanide (HCN) were estimated by correlating the signal intensity of that species with that of a calibrated species with a similar appearance potential through the ratio of their ionization cross sections.¹⁶ The gas composition as a function of height above the surface was reported as a normalized mole fraction by adding the concentrations of the measured species together and dividing each concentration by this total.

Temperature Measurements

Surface temperature was measured by Pt–Pt 13% Rh fine thermocouples with a diameter of 25 μm . These thermocouple wires were carefully welded together under a microscope. Figure 2 illustrates the configuration for measurement of the surface temperature. The thermocouple was placed across the propellant surface, and the thermocouple wires hung about 1 cm down over the edge of the propellant surface with small nuts fastened to the wires to keep the thermocouple bead on the propellant surface. Therefore, the thermocouple was always on the surface throughout the test. During the test, signals generated from thermocouples were recorded on a Nicolet oscilloscope through an amplifier. Then the signals were transferred to a personal computer for further analysis. To estimate the thermal inertia effect, an energy balance was performed. The calculated result for an oscillatory temperature of 4 Hz did not show significant effects on either the amplitude or phase of oscillation.

Results and Discussion

Simultaneous near-surface species and surface temperature measurements were made during the laser-induced decomposition of HMX at a constant heat flux of approximately $30 \pm 5 \text{ W/cm}^2$. All of the tests were performed at atmospheric pressure in argon. After the laser was turned on, a melt layer developed on the propellant surface with no luminous flame. The melt layer showed random dynamic motion without large bubbles during laser-induced decomposition. Several large bubbles were formed on the surface after laser heating was terminated. The bubbling phenomenon lasted approximately 500 ms.

Figure 3 shows the surface species and temperature profiles during the initial stage of the test. In the figure, the x axis represents the time after the laser was turned on. From 0 to 2000 ms, the NO_2 and triazine profiles display intermittent spikes at a frequency of approximately 5 Hz, and the intensities between these spikes were almost zero. The behavior was very similar to chuffing.^{2,3} However, the spikes of pressure observed during the previous tests of chuffing were not found because of the large volume of the combustion chamber. The intermittent production of species was transferred into continuous, but oscillatory, gas evolution at approximately 2000 ms. The temperature profile quickly rose to 500 K after the laser was turned on. Then the temperature remained at about 500 K for approximately 1.6 s until continuous, but oscillatory, gas evolution began. It is interesting to note that the temperature profile did not oscillate with the NO_2 and triazine profiles before continuous, but oscillatory, gas evolution occurred.

Figure 4 displays the temporal species and temperature profiles during the period of continuous, but oscillatory, gas evolution. The average burning rate was $\sim 0.4 \text{ mm/s}$ during this period. In the figure, the species profiles are displayed in normalized mole fraction. The temperature trace was adjusted by 20 ms because of species traveling time between the probe tip and the ion detector. It is interesting that most of the species profiles displayed an oscillation of $4 \pm 0.2 \text{ Hz}$ during the period. The oscillatory frequency during the period was lower than that of NO_2 and triazine during chuffing, and the average burning rate during the period was higher than that during chuffing. The species profiles in Fig. 4 show that NO_2 and CH_2O were the most abundant gas followed by HCN, N_2O , H_2O , and species at mass 28. Only a small amount of NO was observed. NO_2 displayed the largest amplitude followed by CH_2O , N_2O , HCN, NO, triazine, and the species at mass 28. The amplitude for the NO_2 profile was a mole fraction of 0.025, whereas the amplitude for the CH_2O profile was a mole fraction of 0.02. Based on the phase relationship of the species profiles, the measured species could be divided into two groups. NO_2 , HCN, and triazine represent the first group, whereas CH_2O , N_2O , and the species at mass 28 represent the second group. There was a phase difference of 180 deg between these two groups. The phase relationship may indicate

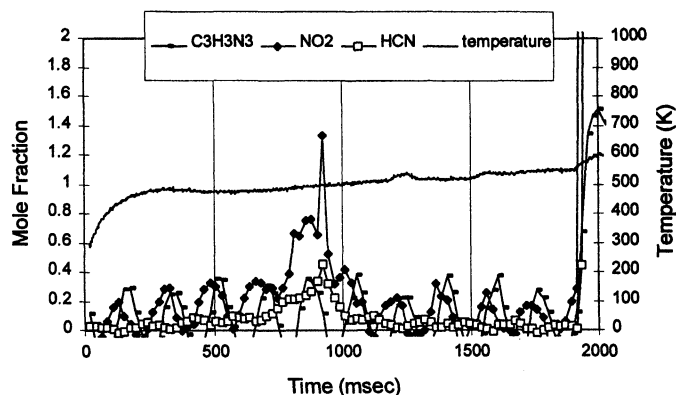


Fig. 3 Simultaneous species and temperature measurements before continuous gas evolution.

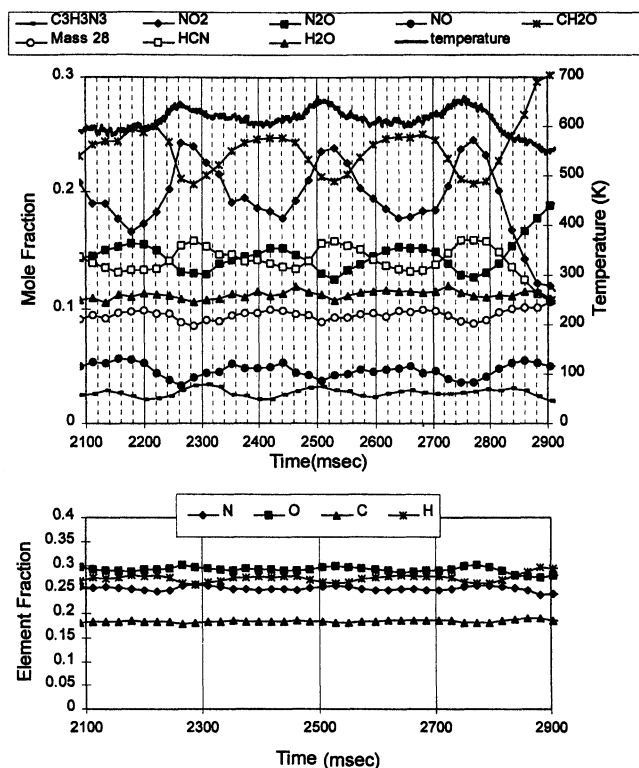


Fig. 4 Simultaneous species and temperature measurements during self-oscillatory burning of HMX with a heat flux of 30 W/cm².

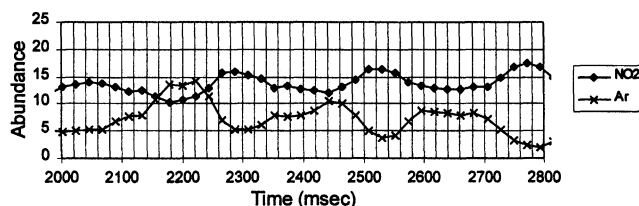
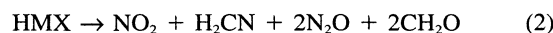


Fig. 5 Comparison of the oscillations of the ambient gas (argon) and NO₂.

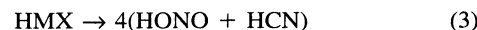
that the production of these two species groups competed in the condensed phase; thus, two competing reaction channels were expected to take place under the test conditions. NO₂ and HCN were the major products for the first reaction channel, whereas CH₂O and N₂O were the major products for the second reaction channel. Because the production of H₂O is normally associated with the major heat-releasing reaction of NO₂ and CH₂O, its production is an indicator of the thermal processes in the condensed phase. The H₂O profile is almost constant from 2.5–2.9 s, and the small peaks of the H₂O profile appear to occur between the peaks of NO₂ and CH₂O. The temperature profile in Fig. 4 also oscillates at a frequency of 4 ± 0.2 Hz. The average temperature and amplitude of the oscillation profile were ~ 633 and 25 K, respectively. The relationship between the temperature and species profiles shows that the temperature profile moves in phase with the first species group. Thus, the first reaction channel became more important as the temperature increased. The bottom of Fig. 4 shows the element balances for those species profiles in the top of Fig. 4. The element fractions of HMX are 0.286 for H, N, and O, as well as 0.143 for C. The N, O, and H balances for the experimental species profiles showed only slight oscillation, and the C balance was 20% higher than the theoretical value. Compared with the element balances obtained for other materials studied with TQMS, these element balances are quite good.

It is observed in Fig. 5 that the profile of argon, the ambient gas, oscillates 180-deg out of phase with NO₂, one of the species in the first group. Because a higher mass flux for a freejet can reduce the concentration of the ambient gas in the center-line of the jet,¹⁷ the relative concentration of the ambient gas could indicate the relative burning rate of the propellant. Thus, an increase in the concentration of argon would indicate a decrease in the burning rate. This result suggests that the first species group became dominant as the burning rate increased.

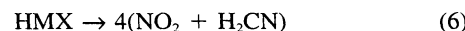
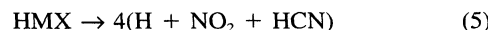
Several researchers have proposed reaction mechanisms for the decomposition of HMX in the condensed phase through experimental observation or theoretical derivation. Behrens and Bulusu¹⁸ published a multipathway mechanism for the decomposition of HMX. Reactions (1) and (2) were the first-order pathways for this mechanism, and reaction (2) was favored at high temperature:



These reaction pathways were derived based on the experiments of thermal decomposition at a low heating rate and low temperature ($<282^\circ\text{C}$). Reactions (3) and (4) for the decomposition of HMX were originally proposed by Melius¹⁹:



After Brill²⁰ conducted a series of experiments at a high heating rate and temperature, he suggested that these two reactions were the global competing reaction branches during the thermal decomposition of condensed-phase HMX. Reaction (3) could be written as reaction (5) or (6):



The competing reaction branches have been adopted in several nitramine models,^{21,22} and these models have made fairly reasonable predictions for the steady-state combustion of nitramine propellants. In related steady-state studies of HMX during laser-assisted combustion, large amounts of HCN, NO₂, CH₂O, and N₂O existed at the burning surface.²³ In general, these results supported the two global reactions because the two reactions would produce significant amounts of these four species. In an attempt to more accurately verify the two global reactions, a higher heat flux was used to understand how the surface temperature affected the surface species under steady-state conditions. Unfortunately, the surface temperature was found to be very insensitive to the heat flux level. Therefore, the surface species as a function of temperature could not be obtained during the steady-state combustion studies of HMX. Brill showed the N₂O/NO₂ ratio as a function of reaction temperature for HMX, and reported that the ratio increased with a decrease in temperature. This indicates that an increase in temperature favored reaction (3), which is qualitatively in line with the relationship between the current measured species and temperature. However, Brill did not report any quantitative effects of temperature on CH₂O and HCN. The two competing reactions other than Behrens and Bulusu's multipathway mechanism were the focus of the current study mainly because these two reactions can qualitatively explain the current results and because the reaction temperature and heating rate for Behrens and Bulusu's experiment are very different from those in the current study.

The top of Fig. 6 displays several species as a function of surface temperature for the oscillatory burning of HMX. These data were taken from the portion of Fig. 4 between 2.5 and

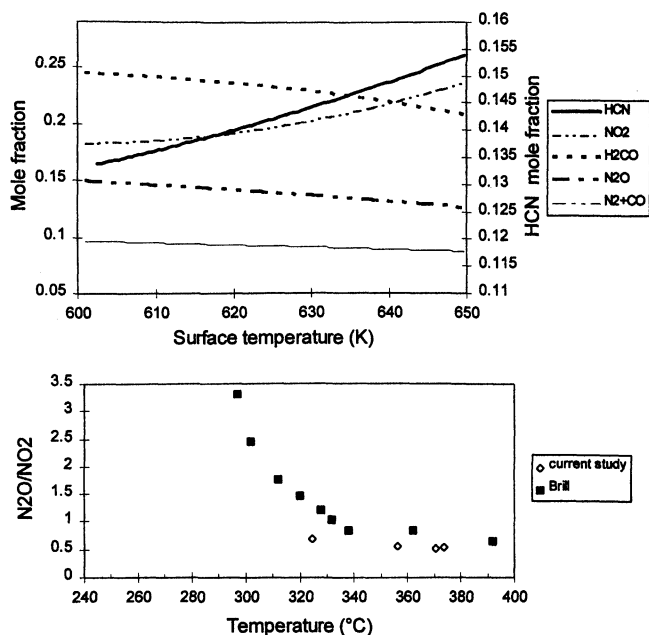


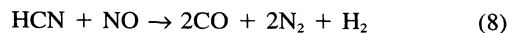
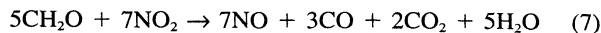
Fig. 6 Temperature dependence as measured by the major species and N_2O/NO_2 ratio.

2.9 s. Apparently, an increase in surface temperature increased the mole fractions of HCN and NO_2 , but decreased the mole fractions of N_2O and CH_2O . The current results further verified temperature effects on HCN and CH_2O , which are the products of the two reaction branches of HMX. However, the rate of increasing HCN was not exactly equal to that of NO_2 , and the rate of decreasing N_2O was not exactly equal to that of CH_2O . Thus, the experimental results qualitatively supported the relationship between temperature and the products of these two equations, but could not quantitatively verify the stoichiometric coefficients of these two equations. These two global reactions also cannot explain the fact that triazine and the species at masses 28 and 43 existed in significant amounts. The results indicate that the two global reactions are too simple to describe the condensed phase chemistry, even though the results qualitatively confirm the two reactions.

The species profiles in Fig. 4 show that triazine still existed at a detectable level, even at a surface temperature as high as 630 K. The average surface temperature was close to the surface temperature (633 K) observed under self-sustained combustion at 1 atm.²⁴ Thus, the reactions associated with the production of triazine in the current condensed phase study may be applicable to steady-state combustion at atmospheric pressure. Previous work under steady-state conditions²⁵ also showed that the reactions related to triazine could be important in the gas phase during laser-assisted combustion. Fifer²⁶ proposed that one molecule of triazine may decompose to form three molecules of HCN. If one molecule of triazine was counted as three molecules of HCN, the total mole fraction of HCN was very close to the mole fraction of NO_2 in the current study. This implies that NO_2 did not quantitatively match HCN simply because triazine did not decompose into HCN. The presence of triazine may result in different gas-phase chemistry from HCN.

The bottom of Fig. 6 shows the comparison of the N_2O/NO_2 ratios between the current study and Brill's study. The measurement technique used in the current study was entirely different from that in Brill's study. In addition, Brill's data were obtained under transient conditions, whereas the current data were measured for a *steady-state* oscillatory condition. Nevertheless, the comparison shows that the N_2O/NO_2 ratio in the current study is only slightly smaller than that in Brill's work.

Oscillations of the width of the reaction zones in the gas phase could cause oscillatory species profiles. Previous TQMS,²³ uv-visible absorption,²⁷ and planar laser-induced fluorescence²⁸ measurements showed the primary and secondary reaction zones in the gas phase during laser-assisted combustion of HMX. In the primary reaction zone, reaction (7) was dominant, whereas in the secondary reaction zone, reaction (8) was prevailing:



Time-of-flight mass spectrometry measurements²⁹ also showed two similar reaction zones during the self-sustained combustion of HMX. Oscillation of the width of the secondary reaction zone has been observed with an external sinusoidal heat flux.³⁰ During this oscillation, a phase difference of 180 deg was found between the profiles of products (CO and N_2) and reactants (HCN and NO) of reaction (8). In the same fashion, oscillation of the width of the primary reaction zone was expected to show a phase difference of 180 deg between the CH_2O and NO profiles. The phase relationship among species could be used as a tool to examine whether or not oscillations of the width of reaction zones existed. Korobeinichev et al.²⁹ showed species profiles with an ~ 180 -deg phase difference between the profiles of $m/z = 30$ and 28; thus, oscillation of the width of the secondary reaction zone was expected to cause these oscillatory species profiles. However, the current results did not show such a phase relationship among species profiles. On the other hand, the current oscillatory species profiles could be quantitatively explained by the two competing reactions in the condensed phase. Thus, it is believed that the observed oscillations were a result of the condensed-phase reactions rather than oscillations of the width of the gas-phase reaction zones.

Kooker and Nelson⁷ showed that the large exothermic heat release in the condensed phase induced self-oscillatory burning without the assistance of external radiation. Their calculation was based on the assumption that the surface reaction zone is infinitesimally thin and that the gasification process is one-step. They also found that the oscillatory amplitude decreased with a decrease in the surface heat release, and that when the surface heat release was below a specific value, self-oscillatory burning could not occur. Based on the same assumption, De Luca et al.³¹ introduced two variables, defined, respectively, in terms of burning surface and gas-phase properties:

$$a \equiv \left[(T_s - T_1) \frac{\partial \ln m_s}{\partial T_s} \right]_{\bar{r}_i} \quad (9)$$

$$b \equiv \left[\left(\frac{\partial \tilde{q}_{g,s}}{\partial m_s} + Q_s \right) \frac{\partial \ln m_s}{\partial T_s} \right]_{\bar{r}_i} - \frac{c_g - c_c}{c_c} \quad (10)$$

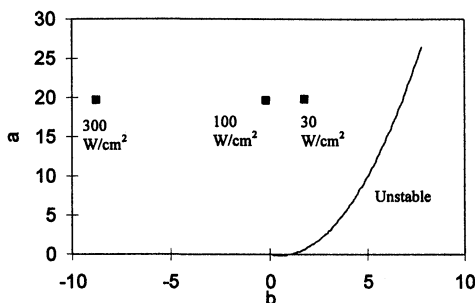
where T_s is the surface temperature, T_1 is the initial temperature, c_g is the specific heat for the gas phase, c_c is the specific heat for the condensed phase, m_s is the burning rate, Q_s is the surface heat release, and $\tilde{q}_{g,s}$ is the heat feedback from the gas phase. $c_g = 0.35$ cal/g K and $c_c = 0.35$ cal/g K can be found in Ref. 32. Then, the intrinsic stability boundary can be described as:

$$a = (b/2)(b - 1) \quad (11)$$

Equation (11) can be used to determine the stability boundary during self-sustained or laser-assisted combustion. If $a < b(b - 1)/2$, burning is not stable. Although the term of the external heat flux is not in the a or b , these two parameters implicitly depend on the radiant flux intensity. As in Kooker and Nelson's model,⁷ the surface heat release included in a

Table 1 Burning rate, surface temperature, and surface heat release as a function of heat flux

Heat flux, W/cm ²	Burning rate, mm/s	Surface temperature, K	Surface heat release rate, ^a W/cm ²	Surface heat release, ^a J/g	<i>a</i>	<i>b</i>
30	0.4	633	7.7	112	19.8	1.7
100	0.9	647	-2.5	-15	19.7	-0.2
300	1.2	652	-143.4	-664	19.7	-8.8

^aSurface heat release is positive if exothermic.**Fig. 7** Intrinsic stability of HMX with an external heat flux.

and *b* was a dominant factor for stability. *a* and *b* for the current study could be derived from the measured surface temperature and burning rate equation along with an estimate of the surface heat release. The burning rate equation is described in the following form:

$$m_s = A \exp(-E_a/RT) \quad (12)$$

$E_a = 47$ kcal/mole was readily obtained, based on the measured temperatures and burning rates from the current study. The surface heat release can be obtained through the one-dimensional energy equation using the measured surface temperature and external heat flux as known values. With *a* and *b* as a function of the external heat flux, stability at a given heat flux can be determined through Eq. (11)

Table 1 shows these two parameters and the surface heat release as a function of heat flux. The values of *a* and *b* suggest that burning is stable at the heat fluxes from 30 to 300 W/cm². Figure 7 shows the stability boundary and an effect of radiation on intrinsic stability for HMX. The data point moves toward the unstable region as heat flux decreases. The trend was indeed in line with the experimental observation. However, these two parameters predict stable burning at a heat flux of 30 W/cm², which did not agree with the observed oscillatory burning at a heat flux of 30 W/cm². It appears that the previous mechanism cannot exactly predict the experimental results. In an effort to explain the current results, additional effects were considered in the condensed phase.

Brill and Brush³³ found that multiple-step reactions were involved in the condensed phase decomposition of HMX, even though their results were consistent with the two global competing reactions in the condensed phase. They also mentioned that as the concentration of residue increased in the condensed phase, the HMX decomposition accelerated. Behrens³⁴ reported that the residue and CH₂O were autocatalytic. Thynell et al.²² used a numerical model to simulate the experimental results of Brill and Brush, using multiple-step condensed phase reactions. They assumed that the products from the two competing reactions were dissolved in the liquid layer. Therefore, NO₂ and CH₂O could build up in the liquid layer before an exothermic runaway occurred. The previous studies suggested that the reactions in the HMX condensed phase were multiple steps, and some species could build up in the condensed phase. The species buildup could induce certain condensed phase reactions or accelerate condensed phase reactions.

To illustrate how multiple-step reactions in the condensed phase might affect oscillatory burning, consider that the condensed phase of HMX is controlled by a two-step reaction: (A) $\text{HMX} \rightarrow \text{HMX}_{(\text{int})}$ and (B) $\text{HMX}_{(\text{int})} \rightarrow \text{gas-phase products}$, where $\text{HMX}_{(\text{int})}$ represents intermediate species. Reaction (A) is endothermic, whereas reaction (B) is exothermic. With this model, the total heat release from HMX to gas-phase products still can be consistent with the experimental data at a surface of ~ 633 K, which indicates a very small exothermicity or even endothermicity in the condensed phase. Initially, reaction (A) can build up the concentration of $\text{HMX}_{(\text{int})}$ in the condensed phase before a large amount of reaction (B) occurs. When the concentration of $\text{HMX}_{(\text{int})}$ and temperature in the condensed phase reach a critical value, a large amount of reaction (B) will momentarily occur; thus, a large amount of heat associated with reaction (B) will be released in the condensed phase. The heat can easily drive the temperature of the reaction zone to a higher level. After the amount of $\text{HMX}_{(\text{int})}$ is almost completely consumed, reaction (B) will slow and the temperature will drop to a lower level. Thus, based on a two-step condensed phase reaction, self-oscillatory burning may occur even when the global surface heat release is not highly exothermic. In other words, self-oscillatory burning is induced by the transient condensed phase heat release instead of the global condensed phase heat release. Because the concentration of $\text{HMX}_{(\text{int})}$ in the condensed phase is crucial to self-oscillatory burning, the time scale of the species buildup can possibly affect the frequency of oscillation. Therefore, both thermal relaxation time and chemical processes in the condensed phase could control the frequency of oscillatory burning; a different model from that of previous researchers. In fact, a numerical calculation based on the previous mechanism could not predict the frequency of oscillatory burning well.⁸ Though the other models such as incomplete combustion are available in literature,^{35,36} these models also cannot explain these data. The chemical processes in the condensed phase may be the reason why the purely thermal model could not predict the frequency of oscillation.

Self-oscillatory burning for HMX was observed at a heat flux of 30 ± 5 W/cm², but not at heat fluxes above 100 ± 10 W/cm². To explain this behavior, an analysis of global heat release was performed. Table 1 shows that the surface heat release becomes more endothermic with an increase in external heat flux and surface temperature. Comparison of the external heat flux and surface heat release shows that the external heat flux dominates in the surface reaction zone at heat fluxes ranging from 30 to 300 W/cm². Table 2 shows the analyses of chemical kinetics for the surface heat release. The rate constants as a function surface temperature were derived based on Eqs. (13) and (14), which are the rate constants for reactions (3) and (4):

$$k = 10^{16.5} \exp(-44,100/RT) \quad (13)$$

$$k = 10^{13.0} \exp(-34,400/RT) \quad (14)$$

The activation energy and pre-exponential factor can be found in Ref. 20. It is evident that the surface heat release decreases with an increase in temperature. The surface heat release is based on the global reactions (3) and (4), which are endothermic.

Table 2 Rate constants and heat release as a function of the surface temperature

Surface temperature, K	Rate constant for reaction (3), 1/s	Rate constant for reaction (4), 1/s	Heat release, ^a J/g
600	2.73	2.95	-114.6
630	15.91	11.66	11.8
650	47.04	27.16	86.5

^aHeat release is negative if exothermic.

mic (38 kcal/mole) and exothermic (-50 kcal/mole), respectively. Although several reactions other than these two reactions certainly took place in the condensed phase, the mole fractions of species produced by these reactions were relatively constant. Thus, even if all of the reactions in the condensed phase were considered for the surface heat release, the surface release still would decrease with an increase in heat flux. In addition to the surface heat release, Table 2 shows information regarding which reaction causes the endothermic surface heat release. Because the increasing heat flux increases the surface temperature, reaction (3) is more dominant at a higher heat flux. Thus, the analysis of global heat release can be used to explain the relationship between the external heat flux and oscillatory burning, but further analysis was needed to predict the exact boundary of stability. As long as the increasing rate of the external heat flux is higher than that of the surface heat release, it is most likely that oscillatory burning will diminish as external heat flux increases.

Conclusions and Summary

Self-oscillatory burning of HMX was observed at atmospheric pressure with a constant heat flux of 30 ± 5 W/cm². The surface species and temperature with an average temperature of ~633 K oscillated at frequencies of 4 ± 0.2 Hz. The mole fractions of NO₂, HCN, and triazine oscillated in phase with temperature, whereas the mole fractions of N₂O and CH₂O were 180-deg out of phase with temperature. In other words, the mole fractions of NO₂, HCN, and triazine increased with an increase in temperature, whereas the mole fractions of N₂O and CH₂O decreased with an increase in temperature. This was qualitatively in line with the accepted global reaction branches in the condensed phase of HMX. Thus, the observed oscillation should be related to the condensed phase processes, not to the gas phase reactions. As the heat flux was increased to 100 W/cm², oscillatory burning was not observed. It is very difficult to explain the current experimental results using the purely thermal model, based on the assumption that the surface reaction zone is infinitesimally thin and that the gasification process is one-step. Multiple-step reactions in the condensed phase may be the reason for the discrepancy between experimental data and the theory of thermal wave relaxation time. However, only detailed modeling can confirm this explanation.

The current results demonstrated that oscillatory burning could exist even with a constant external heat flux. Because the coupling between the condensed phase and gas phase was very complicated and had many unknowns, the current data represent a simple case that still includes the coupling of thermal and chemical processes in the condensed phase during oscillatory burning. Understanding of this coupling could be a good start to understand the more complete interaction between the condensed phase and gas phase.

References

- Huggett, C., Bartley, C. E., and Mills, M., *Solid Propellant Rocket*, Princeton Univ. Press, Princeton, NJ, 1960.
- Huffington, J. D., "The Burning and Structure of Cordite," *Transactions of the Faraday Society*, Vol. 47, No. 8, 1951, pp. 864-876.
- Huffington, J. D., "The Unsteady Burning of Cordite," *Transactions of the Faraday Society*, Vol. 50, No. 9, 1954, pp. 942-952.
- Clemmow, D. M., and Huffington, J. D., "An Extension of the Theory of Thermal Explosion and Its Applications to the Oscillatory Burning of Explosives," *Transactions of the Faraday Society*, Vol. 52, No. 3, 1956, pp. 385-396.
- Librovich, V. B., and Makhviladze, G. M., "One Limiting Scheme for the Propagation of a Pulsating Exothermic Reaction Front in a Condensed Medium," *Journal of Applied Mechanics and Technical Physics*, Vol. 15, No. 6, 1974, pp. 107-116.
- Yount, R. A., and Angelus, T. A., "Chuffing and Nonacoustic Instability Phenomena in Solid Propellant Rockets," *AIAA Journal*, Vol. 2, No. 7, 1964, pp. 1307-1313.
- Kooker, D. E., and Nelson, C. W., "Numerical Solution of Solid Propellant Transient Combustion," *Journal of Heat Transfer*, Vol. 101, No. 2, 1979, pp. 359-364.
- Bruno, C., Riva, G., Zanotti, C., Donde, Grimaldi, C., and De Luca, L., "Oscillatory Burning of Composite Propellants near Pressure Deflagration Limit," *Acta Astronautica*, Vol. 12, No. 5, 1985, pp. 351-360.
- De Luca, L., "Theory of Nonsteady Burning and Combustion Stability of Solid Propellants by Flame Models," *Nonsteady Burning and Combustion Stability of Solid Propellants*, edited by L. De Luca, E. W. Price, and M. Summerfield, Vol. 143, Progress in Astronautics and Aeronautics, AIAA, Washington, DC, 1992, pp. 519-600.
- Galfetti, L., Riva, G., and Bruno, C., "Numerical Computations of Solid-Propellant Nonsteady Burning in Open or Confined Volumes," *Nonsteady Burning and Combustion Stability of Solid Propellants*, edited by L. De Luca, E. W. Price, and M. Summerfield, Vol. 143, Progress in Astronautics and Aeronautics, AIAA, Washington, DC, 1992, pp. 643-687.
- Zanotti, C., and Carretta, U., "Self-Sustained Oscillatory Burning of Solid Propellants: Experimental Results," *Nonsteady Burning and Combustion Stability of Solid Propellants*, edited by L. De Luca, E. W. Price, and M. Summerfield, Vol. 143, Progress in Astronautics and Aeronautics, AIAA, Washington, DC, 1992, pp. 399-439.
- Davidson, J., and Beckstead, M. W., "A Three-Phase Model of HMX Combustion," *26th Symposium (International) on Combustion*, The Combustion Inst., Pittsburgh, PA, 1996, pp. 1989-1996.
- Oberg, C. L., "Combustion Instability: The Relationship Between Acoustic and Nonacoustic Instability," *AIAA Journal*, Vol. 6, No. 2, 1968, pp. 265-271.
- Culick, F. E. C., "Some Nonacoustic Instabilities in Rocket Chambers Are Acoustic," *AIAA Journal*, Vol. 6, No. 7, 1968, pp. 1421-1423.
- Tang, C.-J., Lee, Y., and Litzinger, T. A., "A Study of Gas-Phase Processes During the Deflagration of RDX Composite Propellants Using a Triple Quadrupole Mass Spectrometer," *31st JANNAF Combustion Meeting*, CPIA Publ. 620, Vol. 2, 1994, pp. 307-316.
- Bobeldijk, M., Van der Zande, W. J., and Kistemaker, P. G., *Journal of Chemical Physics*, Vol. 179, No. 2, 1994, pp. 125-130.
- Kuo, K. K., *Principles of Combustion*, Wiley, New York, 1986.
- Behrens, R., Jr., and Bulusu, S., "Recent Advances in the Thermal Decomposition of Cyclic Nitramines," *Proceedings of Materials Research Society Symposium*, Vol. 296, Materials Research Society, 1993, pp. 13-24.
- Melius, C. F., "Thermochemical Modeling: I. Application to Decomposition of Energetic Materials," *Chemistry and Physics of Energetic Materials*, edited by S. N. Bulusu, Kluwer, Dordrecht, The Netherlands, 1990, pp. 21-49.
- Brill, T. B., "Multiphase Chemistry Considerations at the Surface of Burning Nitramine Monopropellants," *Journal of Propulsion and Power*, Vol. 11, No. 4, 1995, pp. 740-751.
- Liau, Y.-C., and Yang, V., "Analysis of RDX Monopropellant Combustion with Two-Phase Subsurface Reaction," *Journal of Propulsion and Power*, Vol. 11, No. 4, 1995, pp. 729-739.
- Thynell, S. T., Gongwer, P. E., and Brill, T. B., "Condensed-Phase Kinetics of Cyclotrimethylenetrinitramine by Modeling the T-Jump/Infrared Spectroscopy Experiment," *Journal of Propulsion and Power*, Vol. 12, No. 5, 1996, pp. 933-939.
- Tang, C.-J., Lee, Y., Kudva, G., and Litzinger, T. A., "A Study of the Gas Phase Chemical Structure During CO₂ Laser Assisted Combustion of HMX," *32nd JANNAF Combustion Meeting*, CPIA Publ. 638, Vol. 1, 1995, pp. 107-118.
- Zenin, Z., "HMX and RDX: Combustion Mechanism and Influence on Modern Double-Base Propellant Combustion," *Journal of Propulsion and Power*, Vol. 11, No. 4, 1995, pp. 752-758.
- Tang, C.-J., "A Study of the Steady Chemical Structure of HMX Propellants and Combustion Response to Oscillatory Radiant Heat Flux," Ph.D. Dissertation, Pennsylvania State Univ., University Park, PA, 1997.
- Fifer, R. A., "A Chemistry of Nitramine Ester and Nitramine Pro-

pellants," *Fundamentals of Solid Propellant Combustion*, edited by K. K. Kuo and M. Summerfield, Vol. 90, Progress in Astronautics and Aeronautics, AIAA, New York, 1984, pp. 177-237.

²⁷Hanson-Parr, D., and Parr, T., "Absorption Measurements in Propellant Flames," *28th JANNAF Combustion Meeting*, CPIA Publ. 573, Vol. 2, Oct. 1991, pp. 369-378.

²⁸Parr, T., and Hanson-Parr, D., "RDX, HMX, and XM39 Self-Deflagration Flame Structure," *32nd JANNAF Combustion Meeting*, CPIA Publ. 631, Vol. 1, 1995, pp. 429-437.

²⁹Korobeinichev, O. P., Kuibida, L. V., Paletsky, A. A., and Chernov, A. A., "Study of Solid Propellant Flame Structure by Mass-Spectrometric Sampling," *Combustion Science and Technology*, Vols. 113-114, 1996, pp. 557-571.

³⁰Tang, C.-J., Kudva, G., Lee, Y., and Litzinger, T. A., "A Study of the Combustion Response of the HMX Monopropellant to Sinusoidal Laser Heating," *33rd JANNAF Combustion Meeting*, CPIA Publ. 653, Vol. 1, 1996, pp. 159-168.

³¹De Luca, L., Di Silvestro, R., and Cozzi, F., "Intrinsic Combustion Instability of Solid Energetic Materials," *Journal of Propulsion and Power*, Vol. 11, No. 4, 1995, pp. 804-815.

and Power, Vol. 11, No. 4, 1995, pp. 804-815.

³²Li, S. C., and Williams, F. A., "Effects of Two-Phase Flow in a Model for Nitramine Deflagration," *Combustion and Flame*, Vol. 80, Nos. 3, 4, 1990, pp. 329-349.

³³Brill, T. B., and Brush, P. J., "Condensed Phase Chemistry of Explosives and Propellants at High Temperature: HMX, RDX and BAMO," *Philosophical Transactions of the Royal Society of London, Series A: Mathematical and Physical Sciences*, Vol. 339, No. 1631, 1992, pp. 377-385.

³⁴Behrens, R., Jr., "Thermal Decomposition of Energetic Materials. Temporal Behaviors of the Rates of Formation of the Gaseous Pyrolysis Products of HMX," *Journal of Physical Chemistry*, Vol. 94, No. 7, 1990, pp. 6706-6718.

³⁵Schoyer, H. F. R., "Incomplete Combustion: A Possible Cause of Combustion Instability," *AIAA Journal*, Vol. 21, No. 8, 1983, pp. 1119-1126.

³⁶Williams, F. A., and Lengelle, G., "Simplified Model for Effect of Solid Heterogeneity on Oscillatory Combustion," *Astronautica Acta*, Vol. 14, No. 2, 1969, pp. 97-118.

Tactical Missile Propulsion

G.E. Jensen and David W. Netzer, editors

With contributions from the leading researchers and scientists in the field, this volume is a compendium of the latest advances in tactical missile propulsion. The objectives of the book are to provide today's designer with a summary of the advances in potential propulsion systems as well as provide a discussion of major design and selection considerations. Authors were chosen for their demonstrated knowledge of and excellence in their respective fields to ensure a complete and up-to-date summary of the latest research and developments.

CONTENTS:

Introduction • Design Concepts and Propulsion Definition • Liquid Rockets • Solid Rocket Motor Design • Solid Propellant Grain Structural Design and Service Life Analysis • Solid Rocket Nozzle Design • Solid Rocket Case Design • Solid Rocket Plumes • Insensitive Munitions for Solid Rockets • Gas Turbines • Liquid Fueled Ramjets • Ducted Rockets • Solid Fuel Ramjets • High Mach Number Applications

1996, 650 pp, illus, Hardcover

ISBN 1-56347-118-3

AIAA Members \$89.95

List Price \$104.95



American Institute of Aeronautics and Astronautics

Publications Customer Service, 9 Jay Gould Ct., P.O. Box 753, Waldorf, MD 20604
Fax 301/843-0159 Phone 800/682-2422 8 a.m. - 5 p.m. Eastern

CA and VA residents add applicable sales tax. For shipping and handling add \$4.75 for 1-4 books (call for rates for higher quantities). All individual orders, including U.S., Canadian, and foreign, must be prepaid by personal or company check, traveler's check, international money order, or credit card (VISA, MasterCard, American Express, or Diners Club). All checks must be made payable to AIAA in U.S. dollars, drawn on a U.S. bank. Orders from libraries, corporations, government agencies, and university and college bookstores must be accompanied by an authorized purchase order. All other bookstore orders must be prepaid. Please allow 4 weeks for delivery. Prices are subject to change without notice. Returns in sellable condition will be accepted within 30 days. Sorry, we can not accept returns of case studies, conference proceedings, sale items, or software (unless defective). Non-U.S. residents are responsible for payment of any taxes required by their government.